Thermal Analysis of Trapped Hydrogen in Pure Iron

W. Y. CHOO and JAI YOUNG LEE

The relative amount of trapped hydrogen and the activation energy for its evolution from various lattice defects in iron were calculated by monitoring the pressure change caused by release of hydrogen from charged specimens heated at uniform heating rates. Hydrogen release peaks were observed at 385 K, 488 K, and 578 K, respectively, when the hydrogen charged specimen were heated at 2.6 K per minute. Analysis suggests that the peak at 385 K corresponds to hydrogen release from grain boundaries, and the peak at 488 K corresponds to release from dislocations, while the peak at 578 K results from release from microvoids. The activation energies for evolution of trapped hydrogen were determined experimentally from measured peak temperatures at different heating rates and were found to be 17.2 KJ/mol, 26.8 KJ/mol, and 35.2 KJ/mol, respectively, in grain boundaries, dislocations, and microvoids. It was also observed that most of hydrogen is trapped on dislocations if the density of specimen is greater than 98.95 pct, and in microvoids if less than 98.95 pct.

I. INTRODUCTION

To understand hydrogen embrittlement of steel, many studies on the role and effect of hydrogen on properties of steel have been carried out recently.[1,2,3] The Fe-H system has been the subject of many thermodynamic and kinetic researches on interstitial solute because of the high hydrogen diffusivity in iron. However, the diffusion mechanism of hydrogen in iron is not clearly understood. As hydrogen embrittlement is closely related to the hydrogen movement in metal, it is very important to verify the exact physical nature of hydrogen behavior in iron, both from an academic viewpoint as well as for practical applications.

Figure 1 shows that the diffusivity of hydrogen in iron deviates markedly from that predicted by the extrapolation of high temperature data taken below 573 K.[4-10] The apparent activation energy in this low temperature region is in the range of 33 to 38 KJ/mol, while in a higher temperature region it is 7.6 KJ/mol. Many researchers[11-17] believe that this phenomenon takes place due to hydrogen being trapped in lattice defects of iron (dislocation, microvoid, and grain boundary) at low temperatures, in as much as the trapping site has a lower energy level than a normal site.

Pressouyre[11] has classified types of trap sites by their physical nature for hydrogen in iron, and suggested vacancies, alloying elements, dislocations, interfaces, and microvoids as possible trap sites. Analyzing the hydrogen diffusivity data in iron, Oriani[12] has estimated trap density and trap-hydrogen interaction energy, and has claimed that interfaces and microvoids are the major trap sites in steels which are not cold worked and cold worked, respectively. Kumnick *et al*[13] in their research of hydrogen permeation in cold worked steel have concluded that dislocation and dislocation debris are trap sites for hydrogen. Riecke[14] has also found that dislocations and dislocation pile-ups act as traps in the measurement of hydrogen diffusivity in hydrogen charged, cold worked, and recrystallized iron specimen. Pressouyre and Bernstein[15] have found that TiC traps hydrogen irreversibly. In this study they have analyzed permeation transients. As a basic work, Wada *et al*[16] observed

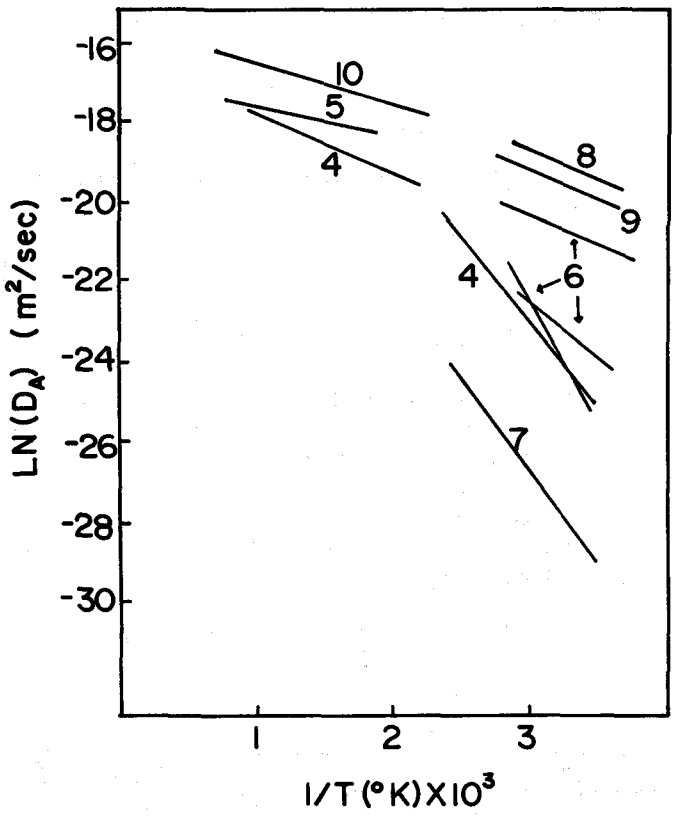

Fig. 1—Representative data for the apparent diffusivity of hydrogen in α-iron and in ferritic steels.

the change of specific heat through a first order phase transformation at 13.7 K in the hydrogen-iron system and verified that hydrogen is trapped in microvoids as gas molecules. Hargi[17] compared the diffusivity of hydrogen in single crystal and polycrystal iron and concluded that the hydrogen trapping site was at a grain boundary. In order to explain the anomalous behavior of hydrogen in iron, several models have been suggested. One is based on the assumption of equilibrium between trapping sites and normal lattice sites,[12,18] while others are based on the rate of trapping and detrapping from trapping sites.

Although many types of trapping sites have been suggested, no dominant type of trapping site is known, and

W. Y. CHOO, Graduate Student, and JAI YOUNG LEE, Professor, are both with the Department of Materials Science at the Korea Advanced Institute of Science and Technology, Seoul, Korea.

Manuscript submitted January 27, 1981.

ISSN 0360-2133/82/0111-0135$00.75/0

the trapping mechanism has not been clearly established. One purpose of this paper is to identify dominant types of trapping sites and to calculate the activation energies for evolution of trapped hydrogen by applying thermal analysis techniques for a pure Fe-H system. Another purpose is to discuss possible trapping mechanism of hydrogen based on the observed data.

II. THEORY

Figure 2 shows energy levels of interstitial sites (B) and trapping sites (A) where hydrogen resides. The activation energy (E_a) needed to escape from a trapping site is much higher than that of normal lattice diffusion (E_n). As the escape rate of hydrogen from a trapping site is a function of trap activation energy (E_a), it is important to know E_a for each type of trapping site in order to understand the anomalous diffusivity of hydrogen.

The escape reaction of hydrogen from a trapping site is assumed to be:

$$\boxed{H}_{trap} \rightleftarrows \square_{trap} + H_{(in\ lattice)}, \qquad [1]$$

where $\square_{trap}$ is trapping site.

From Eq. [1] one can derive a hydrogen escape rate from a trapping site[21] as

$$\frac{dx}{dt} = A(1 - x)e^{-E_a/RT}, \qquad [2]$$

where $x = \dfrac{N_o - N}{N_o}$.

N_o: the amount of hydrogen in trapping site at $t = 0$
N : the amount of hydrogen in trapping site at $t \neq 0$
T : absolute temperature
R : gas constant
A : constant

To reach a maximum escape rate with uniform heating rate, Eq. [3] should apply, *viz*:

$$\frac{d}{dt}\left(\frac{dx}{dt}\right) = \frac{dx}{dt}\left(\frac{\phi E_a}{RT^2} - Ae^{-E_a/RT}\right) = 0, \qquad [3]$$

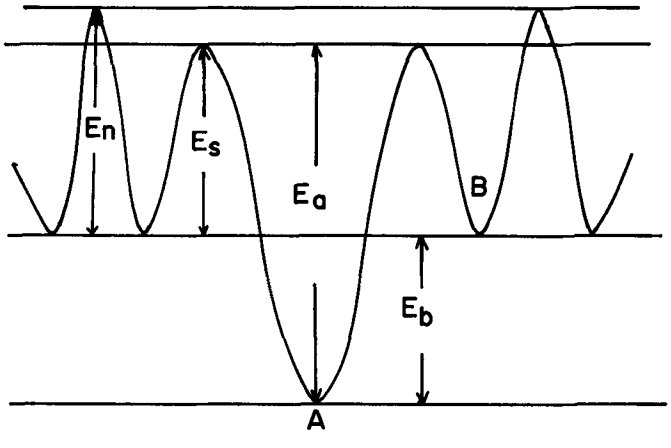

Fig. 2—Model for trapping site. E_n : Diffusion activation energy of hydrogen in normal lattice. E_s : Saddle point energy around the trapping site. E_b : Interaction energy between trapping site and hydrogen. E_a : Trap activation energy ($E_s + E_b$). A : Trapping site. B : Normal lattice site.

where T : $T_o + \phi t$
T_o : initial temperature
ϕ : heating rate

or

$$\frac{E_a\phi}{RT_c^2} = Ae^{-E_a/RT_c}, \qquad [4]$$

where T_c : temperature at which the maximum hydrogen escape occurs. Taking logarithm of Eq. [4] and differentiating with respect to $(1/T_c)$ yields

$$\frac{\partial ln(\phi/T_c^2)}{\partial(1/T_c)} = -E_a/R. \qquad [5]$$

If ϕ and T_c are known, E_a can be easily calculated from the slope of a $ln(\phi/T_c^2)$ *vs* $(1/T_c)$ plot.

III. EXPERIMENTAL PROCEDURE

A. *Sample Preparation*

Electrolytic iron was melted in an induction furnace to a cylindrical form. This ingot was remelted in VAR to remove gaseous elements in the sample. The chemical composition is shown in Table 1. After forging at 1423 K, the ingot was normalized for two hours at 1173 K. To control the amount of lattice defects (dislocations, microvoids, and grain boundaries, and so forth), the specimen was treated as follows:

(1) The dislocation density was varied by cold drawing the sample from zero to 73 pct.

(2) As the amount of microvoids and density are linearly related, portions of the iron with different densities, achieved by 50 to 70 pct drawing, were taken to examine directly the effects of microvoids.

(3) The grain boundary density was adjusted by heat treating the samples between 1073 K to 1173 K for various durations after 60 pct drawing.

B. *Experimental Apparatus and Methods*

Cylindrical specimens (diameter 8 mm, length 15 mm) were charged with hydrogen under 0.2 MPa hydrogen pressure at 673 K for two hours in the apparatus shown in Figure 3, and then quenched into ice water. The hydrogen-charged specimens were transferred to a reaction chamber, Figure 4, and held under vacuum for six hours at room temperature to remove mobile hydrogen, so that only trapped hydrogen remained in the specimen. As each specimen was heated at a uniform heating rate, the trapped hydrogen started to evolve. The time dependence of pressure change in the reaction chamber between 10^{-6} millibar to 5×10^{-3} millibar was checked and used to determine hydrogen evolution rate from trapping sites. This pressure change was monitored by a penning and a thermocouple gauge. Blank tests were done before each run to correct the

Table 1. Chemical Compositions of Specimen

Composition / specimen	C	N	S	P	Ni	Cr	Mo	Si	Mn
Pure iron	—	35	40	—	511	—	—	—	—
wt ppm									

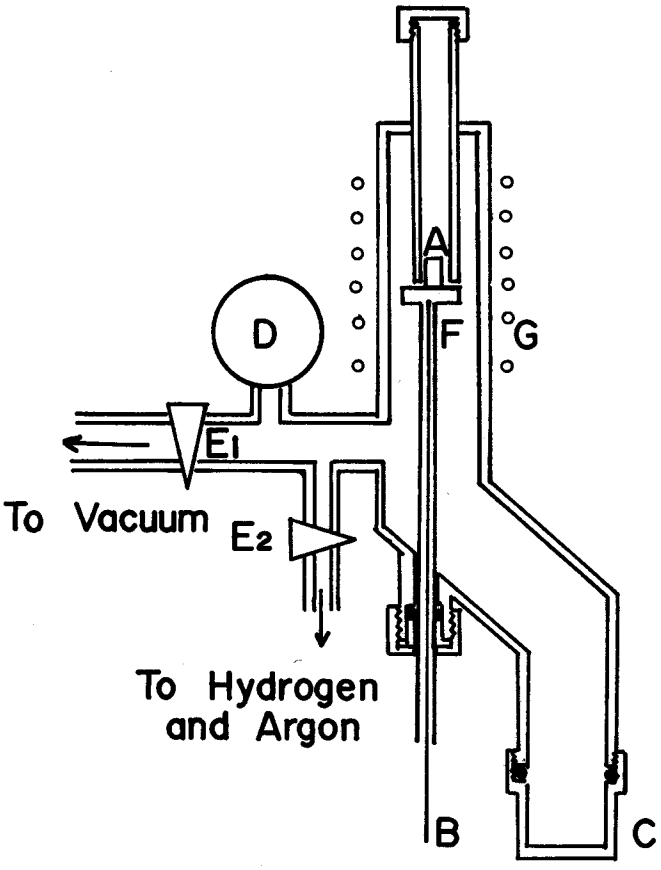

Fig. 3—Schematic diagram of hydrogen charging apparatus. A : specimen, B : thermocouple, C : cooling chamber, D : compound pressure gauge, E_1, E_2 : valves, F : specimen holder, G : furnace.

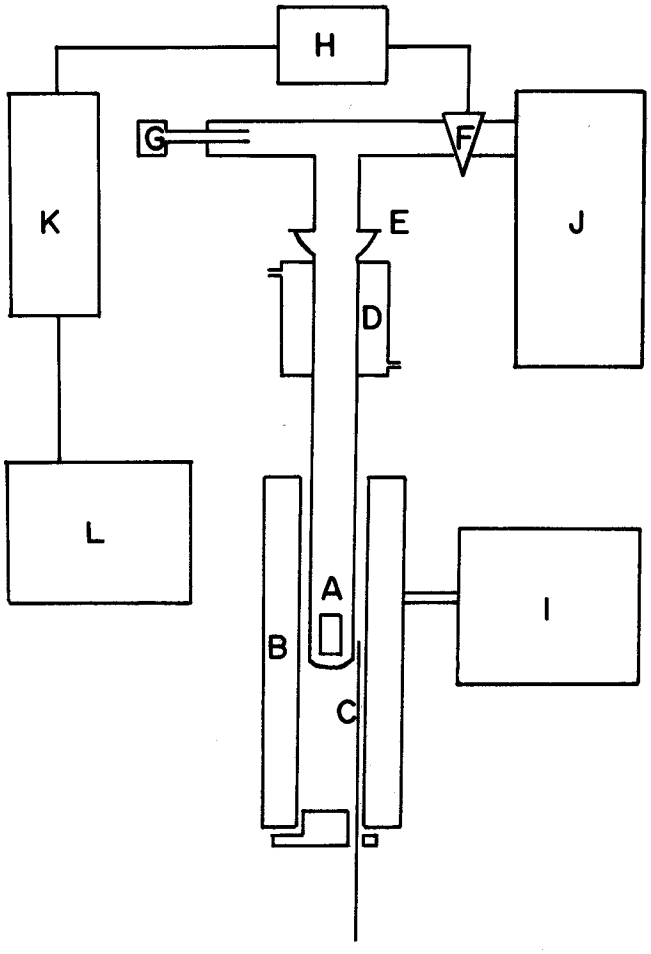

Fig. 4—Schematic diagram of hydrogen thermal analysis apparatus. A : specimen, B : furnace, C : thermocouple, D : water jacket, E : ball and socket joint, F : pneumatic vacuum solenoid valve, G : vacuum senser, H : governer, I : temperature programmer, J : vacuum pump, K : vacuum gauge, L : recorder.

pressure for leakage. The hydrogen evolution rate was expressed by normalizing the rate to 10, and varied from 10^{-6} millibar to 5×10^{-3} millibar per unit time (minute) and unit weight (gram).

The positions and heights of the peaks for the evolution rate *vs* temperature were assumed to be determined by the interaction energy between hydrogen and trapping sites and the amount of hydrogen in trapping sites, respectively. Samples were treated to obtain different amounts of trapping sites. As the heating rates were increased, the position of the peak moved toward the high temperature side as indicated in Eq. [5]. The activation energy of hydrogen evolution from a trapping site was calculated by monitoring change of peak position with variation of heating rates from 8.44 per minute to 1.39 K per minute.

The density of specimen was measured before hydrogen charging by checking the weight of specimen in a microbalance with a sensitivity of 0.1 mg. This gave an indication of the density of microvoids.

IV. RESULTS

A. *The Relation between Lattice Defects and Thermal Analysis Peak*

A typical thermal analysis curve is shown in Figure 5 for a 2.6 K per minute heating rate. After one cycle of thermal analysis, a second was done on the same sample. At this time no peaks were found, indicating that all trapped hydrogen was evolved in the first cycle of analysis. In Figure 5 and Figure 7, three thermal analysis peaks are observed at

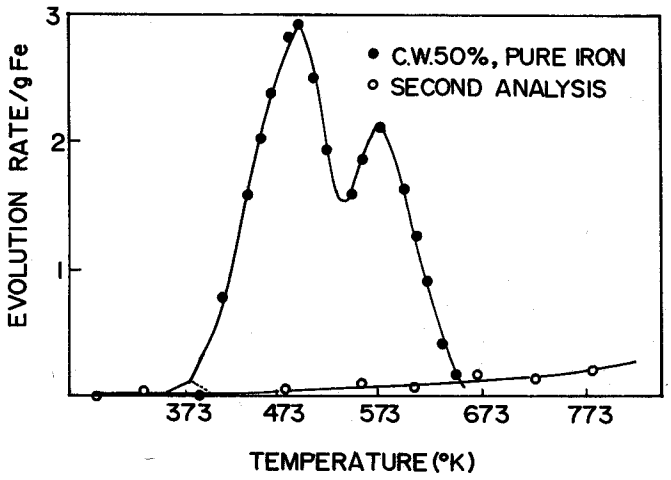

Fig. 5—Typical thermal analysis peaks of hydrogen charged pure iron; second analysis curve is on the same sample.

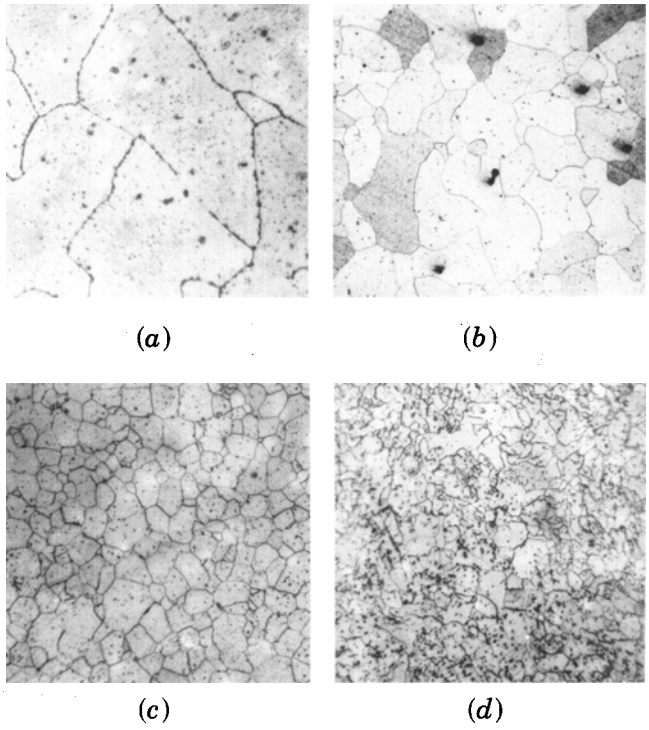

Fig. 6—Microstructures of pure iron. (*a*) ASTM number two, (*b*) ASTM number four, (*c*) ASTM number seven, and (*d*) ASTM number nine. Magnification 65X.

385 K, 488 K, and 578 K, indicating that at least three types of trapping sites exist in a pure Fe-H system. The heights of each peak are different, indicating that the relative amount of hydrogen in each trapping site is different.

(1) *Grain Boundary.* Figure 6 shows microstructures of four different grain size specimens, ranging from ASTM numbers two to nine, used in this work. For these specimens, the dislocation and microvoid densities are kept constant by controlling the degree of cold working; the relative density was 99.85 pct. Thermal analysis peaks with four different grain boundary areas at a heating rate of 2.6 K per minute are shown in Figure 7. As the grain boundary area increases, only the heights of peaks at 385 K increase. That of the other peaks remains unchanged. It is concluded that the peak at 385 K corresponds due to hydrogen trapping in grain boundary.

(2) *Dislocation.* With different degrees of cold working (C. W.), zero to 60 pct, a constant relative density (R. D.) of 99.85 pct, and an initial grain size, ASTM number two, the thermal analysis was done, and the results are given in Figure 8. The heights of peaks at 488 K increase as the degree of cold working increases. This shows that the peak at 488 K is due to an interaction between dislocation and hydrogen. The height of peak increases sharply up to 40 pct C. W., and after that it remains almost constant. In the above experiment the heating rate was 2.6 K per minute.

(3) *Microvoid.* The thermal analysis data for specimens with different relative density (R. D.) are shown in Figure 9. Initial grain size was ASTM number two, and degree of cold working was 50 pct to 70 pct for this experiment. The heating rate was also 2.6 K per minute. While the other peak heights remain uniform, the height of peak at 578 K increases as the relative density decreases. Because the

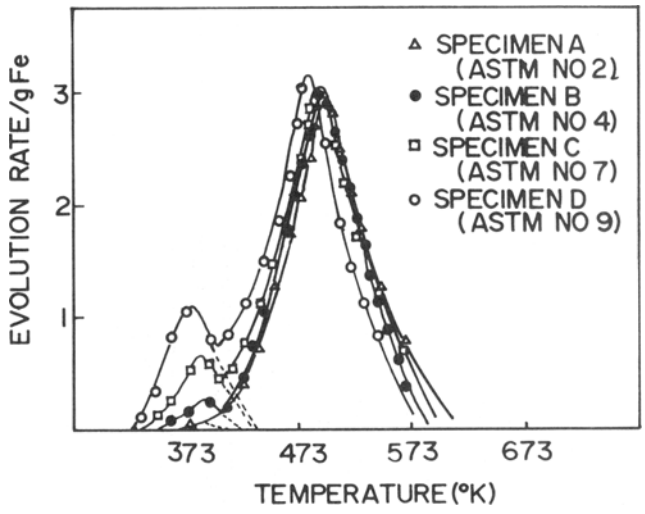

Fig. 7—Dependence of the heights of peaks on the amount of grain boundary area. Heating rate : 2.6 K per minute.

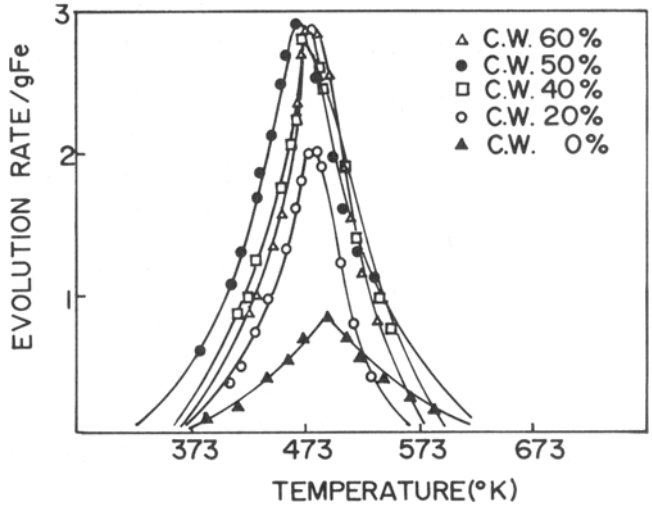

Fig. 8—Dependence of the heights of peaks on the dislocation density. Heating rate : 2.6 K per minute.

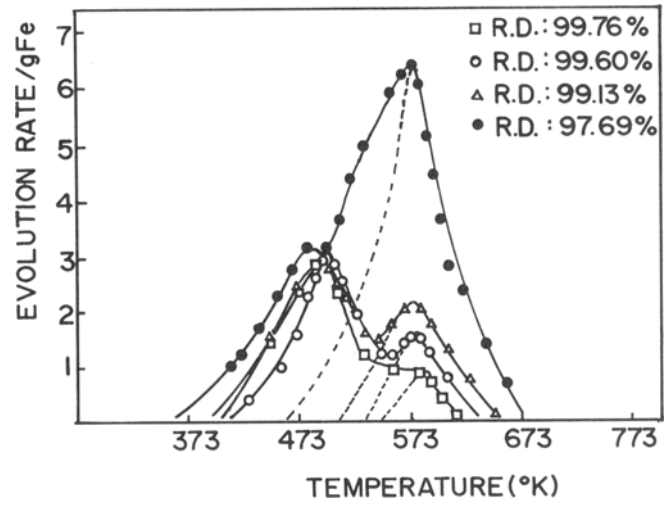

Fig. 9—Dependence of the heights of peaks on the amount of microvoids. Heating rate : 2.6 K per minute.

amount of microvoid is linearly related to the relative density, the peak at 578 K corresponds to a microvoid-hydrogen interaction.

B. *Measurements of Trap Activation Energy*

As the heating rate is increased from 1.39 K per minute to 8.44 K per minute, the peak temperature which corresponds to each lattice defect is increased as shown in Table 2. Using these data and Eq. [5] the trap activation energy (E_a) for hydrogen evolution is obtained, as in Table 2. The activation energy increased in the order of grain boundary, dislocation, and microvoid.

If we assume energy levels around trapping site are located as in Figure 2, the trap activation energy is the sum of the trap-hydrogen interaction energy (E_b) and saddle point energy (E_s). Since the saddle point energy is not known, it is assumed to be the same as the activation energy for normal lattice diffusion (E_n). Then the interaction energy (E_b) is obtained simply by subtracting the activation energy of normal lattice diffusion, (E_n) of 7.6 KJ/mol,[26] from E_a. We found E_b to be 9.6 KJ/mol for grain boundary-hydrogen interaction, 19.2 KJ/mol, dislocation-hydrogen interaction, and 27.6 KJ/mol, microvoid-hydrogen interaction.

V. DISCUSSION

The thermal analysis peak attributed to grain boundaries occurs at 385 K when the specimen is heated at a 2.6 K per minute rate. The interaction energy (E_b) for this peak, 9.6 KJ/mol, is the lowest among the three types of defects. Hargi's[17] data for hydrogen diffusivity in single crystal and polycrystal iron can be compared with our data indirectly. Figure 10 shows the diffusivities above 298 K agree well in both crystals, but below 298 K they deviate from each other. Generally, the diffusivities of hydrogen in iron start to deviate from those from high temperature extrapolation data at about 573 K. From Hargi's results and the fact that the interaction between hydrogen and dislocation or microvoid starts at a much higher temperature, our results on interaction between hydrogen and a grain boundary are within the range of other results.

Table 2. Peak Temperatures of Trapping Site at Various Heating Rates and Trap Activation Energies

Type of Trap	Heating Rate (K Per Minute)	Temperature (K)	KJ/mol
Grain boundary	8.18	435	E_a = 17.2 E_b = 9.6
	5.78	413	
	4.56	399	
	3.77	390	
	3.06	378	
Dislocation	8.44	584	E_a = 26.8 E_b = 19.2
	5.37	548	
	3.88	526	
	2.59	495	
	1.39	471	
Microvoid	8.13	652	E_a = 35.15 E_b = 27.6
	5.27	616	
	3.88	584	
	2.86	573	
	1.39	540	

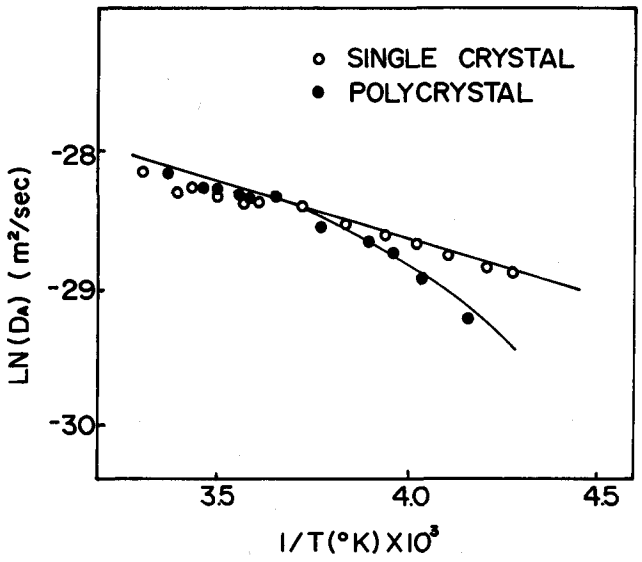

Fig. 10—Temperature dependence of hydrogen diffusivity in single crystal of iron and polycrystal of iron (from Reference 17).

For dislocation-hydrogen interactions in pure iron, the peak temperature is 488 K when heated at a 2.6 K per minute heating rate, and the interaction energy is 19.2 KJ/mol. This value is somewhat smaller than that of Gibala,[22] 26.8 KJ/mol, obtained in his internal friction experiments. The height of peak at 488 K remains constant above 40 pct of cold working. This result agrees well with the report by Keh,[23] that the dislocation density saturates at 40 pct cold working.

For the microvoid-hydrogen interaction in pure iron, the peak temperature is 578 K when heated at a 2.6 K per minute heating rate, and the interaction energy is 27.6 KJ/mol. The physical state of hydrogen in the microvoid is not clearly understood. Some researchers[24,25] claim it exists as a molecule in the microvoid, while others, as adsorbed atoms on the surface of microvoid. Depending on their claim, they suggest different values of hydrogen-microvoid interaction energy. The heat of adsorption of hydrogen on the iron surface of about 133.8 KJ/mol,[18] and heat of solution in iron of 28.8 KJ/mol is reported in the literature.[26] Our measured interaction energy is very close to heat of solution in iron, which suggests a possible molecular state of hydrogen in microvoid. Figure 11 shows a linear relation between peak height and the relative density of sample. That suggests that the amount of trapped hydrogen is linearly related to the volume of microvoid, and not to surface area. This also supports that hydrogen may exist in the microvoid as a molecule.

The saddle point energy (E_s) near the trapping site, shown in Figure 2, is not known. If the interaction energy (E_b) of trapping site-hydrogen is estimated through other experiments such as diffusion or permeation methods, E_s can be calculated using the energy for hydrogen evolution from trapping site (E_a), which is measured as above. This will help us to understand better the physical nature of trapping site.

Comparing relative heights of thermal analysis peaks, relative amount of hydrogen in each trap can be inferred. From Figures 7, 8, and 9, dislocations act as the major trap when the degree of cold working is less than 50 pct, while

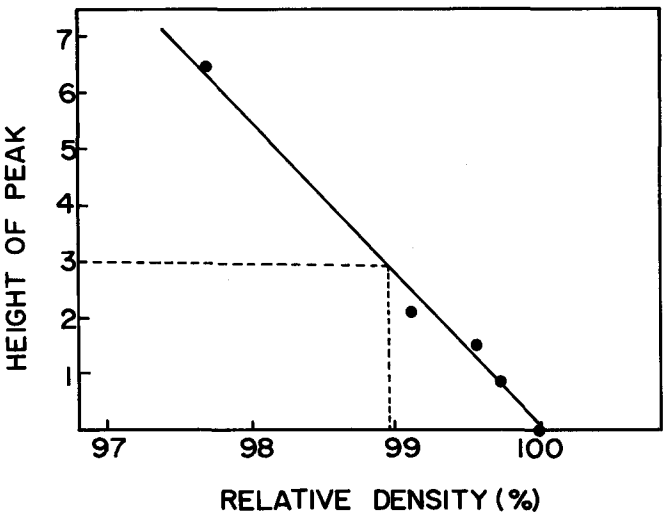

Fig. 11—The relationship between the heights of the peaks at 588 K and the relative density of specimen.

microvoids dominate when cold working is severe and the density of the specimen is altered. Figure 11 shows that the amount of hydrogen corresponding to the maximum height of the dislocation peak is almost the same as that of the microvoids at a relative density of 98.95 pct. The dashed line in Figure 11 shows the transition of major trap sites from dislocation to microvoid. One can conclude that dislocations are a major trap site above 98.95 pct relative density, while below 98.95 pct microvoids are the major trap site.

Oriani *et al*[12,18] assumed a local equilibrium between normal lattice site and trapping site to treat the abnormality of hydrogen diffusion in iron mathematically. According to this assumption, the interaction-energy of trapping site-hydrogen only decides the mass of trapped hydrogen, and hydrogen can easily evolve from the trapping-site, independent of trap energy (E_a), to maintain the local equilibrium. However, our result indicates that a distinct energy is needed to evolve hydrogen from a type of trapping site, in the form of thermal energy. Because of this, the local equilibrium theory is thought to be quite a bold assumption, but the mathematical models of Koiwa[19] and McNabb,[20] which consider trapping and evolution rates from and to trapping site, seem a more proper way to treat the anomalous behavior of hydrogen in iron.

VI. CONCLUSIONS

1. The thermal analysis curve for the Fe-H system (evolution rate *vs* temperature) shows three peaks at 385 K, 488 K, and 578 K. Each peak corresponds to interactions between hydrogen and grain boundaries, dislocations, and microvoids, respectively.
2. The activation energies for hydrogen evolution from trapping sites are 17.2 KJ/mol, 26.8 KJ/mol, and 35.2 KJ/mol for grain boundaries, dislocations, and microvoids, respectively.
3. Above 98.95 pct relative density, the major hydrogen trapping site is dislocation, while below 98.95 pct it is microvoids.
4. It is suggested hydrogen exists in the microvoid as a molecule.

REFERENCES

1. P. Cotterill: *Progress in Materials Science,* Pergamon Press, 1961, vol. 9, p. 201.
2. I.M. Bernstein and A. W. Thompson: *Int. Met. Rev.,* 1976, vol. 212, p. 269.
3. M. Cornet and S. Talbot-Besnard: *Met. Sci.,* 1978, vol. 12, p. 335.
4. E. W. Johnson and M. L. Hill: *Trans. TMS-AIME,* 1960, vol. 218, p. 1104.
5. T. Heuman and D. Primas: *Z. Naturforsch,* 1966, vol. 21A, p. 260.
6. R. C. Frank, D. E. Swerts, and D. L. Fry: *J. Appl. Phys.,* 1958, vol. 29, p. 892.
7. R. M. Barrer: *Trans. Faraday Soc.,* 1940, vol. 36, p. 1242.
8. W. Beck, J. D. M. Bockris, J. McBrren, and L. Nanis: *Proc. Roy. Soc.,* 1966, vol. A209, p. 220.
9. A. J. Kumnick and H. H. Johnson: *Acta. Met.,* 1977, vol. 25, p. 891.
10. N. R. Quick and H. H. Johnson: *Acta. Met.,* 1978, vol. 26, p. 903.
11. G. M. Pressouyre: *Metall. Trans. A,* 1979, vol. 10A, p. 1571.
12. R. A. Oriani: *Acta. Met.,* 1970, vol. 18, p. 147.
13. A. J. Kumnick and H. H. Johnson: *Acta. Met.,* 1980, vol. 28, p. 33.
14. E. M. Riecke: "8th Int. Symp. on Reactivity of Solids", Gothenburg, Sweden, 1976, p. 361.
15. G. M. Pressouyre and I. M. Bernstein: *Metall. Trans. A,* 1978, vol. 9A, p. 1571.
16. Hiroaki Wada and Koshiro Sakamoto: *Scr. Met.,* 1979, vol. 13, p. 573.
17. H. Hargi, Y. Hayashi, and N. Ohtani: *Trans. JIM.,* 1979, vol. 20, p. 349.
18. R. A. Oriani: "Proc. Conf. Fundamental Aspects of Stress Corrosion Cracking", Columbus, Ohio, National Assoc. Corrosion Eng., 1967, vol. 32.
19. M. Koiwa: *Acta. Met.,* 1974, vol. 22, p. 1259.
20. A. McNabb and P. K. Foster: *Trans. TMS-AIME,* 1963, vol. 227, p. 618.
21. H. E. Kissinger: *Analytical Chemistry,* 1957, vol. 29, p. 1702.
22. R. Gibala: *Trans. TMS-AIME,* 1967, vol. 239, p. 1574.
23. A. S. Keh: *Imperfections in Crystals,* Interscience (New York, NY), 1961, p. 233.
24. O. M. Allen-Booth and J. Hewitt: *Acta. Met.,* 1974, vol. 22, p. 671.
25. J. G. Harhai, T. S. Viswanathan, and H. M. Davis: *Trans. ASM. Quart.,* 1965, vol. 58, p. 210.
26. O. D. Gonzalez: *Trans. TMS-AIME,* 1967, vol. 245, p. 607.